Single cells tell their own story: An updated framework for understanding stochastic variations in cell cycle progression in bacteria

Sara Sanders[1, †], Kunaal Joshi[2, †], Petra Levin[1,*], and Srividya Iyer-Biswas[2,3 *]

[1]Department of Biology, Washington University in St. Louis, St. Louis, MO, USA
[2]Department of Physics and Astronomy, Purdue University, West Lafayette, IN, USA
[3]Santa Fe Institute, Santa Fe, NM, USA

[†] Equal contributions
* Corresponence: plevin@wustl.edu and iyerbiswas@purdue.edu

Abstract

Illuminating the molecular mechanisms underlying biological phenomena requires an accurate understanding of the context in which these phenomena occur. Currently, population based experiments frame our understanding of the bacterial cell cycle. Most famously, in 1968 Stephen Cooper and Charles Helmstetter took advantage of their ability to synchronize *E. coli* cells with regard to birth and division using then new technology, the baby machine. Based on baby-machine data, they proposed the existence of two nutrient-dependent growth regimes—slow in which all steps in cell cycle progression are proportional to growth rate and fast in which progression of DNA polymerase plateaus, while new rounds of replication and division remain pegged to growth rate. In the fast regime, the relationship between initiation and division beocome determinant with the latter following the former by a specific amount of time. Still the prevailing model, recent work in single cells reveals a disconnect between the behavior of an idealized average cells (the outcome of population-based analysis) and cell cycle progression in individual cells. To resolve this disconnect, we take an agnostic view of the forces modulating bacterial cell cycle progression and, leveraging extant single cell data, propose a new framework from which to understand this essential process. Significantly, our framework accounts for the stochasticity inherent in biological processes. It is also flexible, providing the ability to assess cell cycle progression independent of medium or genetic background. Using this framework, we test potential explanations for the divergence between single cell growth rate and replication fork elongation rate, identifying limiting reagents as the primary cause of this widespread phenomenon.

Introduction

Proliferation of organisms across the tree of life requires effective coordination of cell growth, DNA replication, and cell division. Coordination is particularly challenging in bacteria, for which population mass doubling times ("MDTs") vary as much as five-fold with nutrient availability. While some bacteria require eukaryotic-like checkpoints to transition between sequential cell cycle processes,[1] others do not have obvious means of coordinating different stages of cell cycle progression beyond the presence of nucleoid occlusion proteins and other factors that prevent division across unsegregated chromosomes. [2–7] In many bacteria, including the model organisms *Escherichia coli* and *Bacillus subtilis*, the initiation and elongation phases of DNA replication overlap at faster growth rates resulting in multiple ongoing rounds of DNA replication on the same chromosomal template.[8,9]

The principles governing bacterial cell cycle progression remain poorly understood, progress

stymied in part by a technologically imposed reliance on population level analysis and idealized average cells. This approach effectively washes out stochastic, cell-to-cell variations in the timing of cell cycle events resulting in models that do not always hold up in single cells. In this perspective, we first provide a brief historical summary of early work on bacterial cell cycle control, with an emphasis on prevailing deterministic models. Next, based on data from recent single cell experiments, we propose a new, agnostic framework from which to understand this widespread phenomenon with a focus on intrinsic stochasticity. We end with example applications of this model and a road map for future work.

The Growth Law: nutrient-imposed growth rate influence multiple aspects of cell cycle regulation

Early work relied on direct visualization of radiolabeled *E. coli* chromosomes to reveal the presence of circular structures. In these autoradiograms, the pattern of radiolabel density indicated that replication initiates and proceeds bidirectionally from a single point, the origin of replication.[10] While slow growing cells contained a maximum of two copies of the origin of replication, faster growing cells contained more than two origin copies with origin number increasing with increases in nutrient imposed growth rate.[3,11–13]

Evaluating the relationship between key physiological parameters and growth rate, Schaechter, Maaløe, and Kjeldgaard determined that *S. tymiphurium* nucleic acid and protein concentration remain constant across a wide range of nutrient imposed growth rates, while size increases exponentially.[3] Later studies confirmed similar relationships in the model bacteria, *E. coli* and *B. subtilis*.[14,15] These findings constitute the classic "nutrient growth law."

While undeniably impactful, early work raised new questions. Most importantly, a unifying mechanism linking the observations of variable origin copy number and the growth law remained elusive. Ultimately, clarification of the relationship between nutrient imposed growth rate and DNA replication required a significant technological advance.

Cooper, Helmstetter, Donachie: a deterministic model of the *E. coli* cell cycle

Addressing the relationship between origin copy number and nutrient imposed growth rate, required a major technological advance permitting both synchronization of bacteria regarding the cell cycle and the ability to assess DNA replication in real time. After a decade of trial and error, Stephen Cooper and Charles Helmstetter successfully engineered the *E. coli* "baby machine."[8] In the baby machine, cells are bound to a filter paper membrane such that daughter cells are eluted immediately after the mother cell divides (hence, the "baby" nomenclature), permitting synchronization. To meet the second requirement, the scientists labeled cells with [14C]-thymidine prior to filter paper binding. Using this technology, relationships between cell age, division time, and DNA synthesis were mathematically related and these models were applied to evaluate mechanistic hypotheses.[8]

Incorporating previous data with results from their baby machine experiments, Cooper and Helmstetter developed a quantiative model of the cell cycle (the "CH model"), relating *E. coli* replication to cell age and mass doubling time (MDT).[8] Still in use today, the CH model posits there are two distinct growth regimes: slow (MDT> 60 minutes) and fast (MDT<60). Single fork replication prevails during slow growth, the initiation and elongation phases varying with nutrient-imposed population growth rate.[8] Under the fast regime, only initiation varies with growth rate. The time required for an average cell to complete a round of replication (C period) and the time between termination and division (D period) both become fixed in the fast regime (with values of

42 and 20 min, respectively, in the early studies on *E. coli* strain B/r).[8] Notably, Cooper and Helmstetter only obtained two sets of data points at MDT > 60 minutes (minimal acetate and minimal succinate)[16] with the remaining datasets obtained at MDTs of 46 minutes or less,[8] significantly limiting resolution at their proposed cut off between the two growth regimes (**Fig. 1**).

Incorporating the early data on origin copy number, DNA content, and cell size, they proposed that cells must initiate new rounds of DNA replication piror to completion of the previous one. This process is known as "multifork replication." Importantly, their model posits that replication transitions from single fork replication (≤2 forks) to multifork replication (6+ forks) such that the degree of multifork replication corresponds to the growth rate.[8] They further propose that the transition to multifork replication is driven by the requirement for replication to keep pace with growth rate—multifork replication as a mechanism to overcome the C period plateau, and apply the mathematical simplification that all forks proceed at the same rate.

Focusing specifically on the fast regime, Cooper and Helmstetter inferred that 1) division always follows initiation by C+D minutes and 2) multifork replication is a consequence of C > generation time (time between cell birth and subsequent cell division). In the CH model, multifork replication is adaptive, ensuring that at least one round of replication will be completed prior to division despite the fixed nature of C-period, permitting distribution of complete chromosomes to daughter cells.

In a follow-up analysis, William Donachie combined the CH model with the nutrient growth law to infer that during fast growth, replication initiation occurs at a constant cell size ("initiation mass").[17] This model holds experimentally in *E. coli* and *Salmonella* and even extends to the Gram-positive model organism, *Bacillus subtilis*.[14,15,18–24] At the molecular level, constant initiation mass is achieved through the initiator protein DnaA, which acts as the primary factor coupling replication initiation to achievement of a specific size in *E. coli.*[25–27] DnaA concentration is relatively constant across growth rates, and recent work indicates that *E. coli* requires a threshold number of DnaA molecules to initiate a new round of replication. Briefly, given constant concentration, the number of DnaA molecules increase with cell growth, reaching threshold numbers at a specific cell size. Detailed information on DnaA and its regulation is reviewed elsewhere.[28–33]

When applied to population level analyses of wild type cells, this model provides an accurate, but fuzzy, view of the bacterial cell cycle. Molecular biologists (including PAL and SS) rely on a variation of the CH model equations to infer DNA replication rates from the relative quantities of origin- versus terminus-proximal chromosomal DNA by qPCR.[9,28,34,35] While these equations serve as useful tools, they do not clarify mechanism at the molecular levels. For example, multiple reports describe mutant strains that display a C-period significantly shorter than that in wild type cells, however, the forces underlying this increase in progression of the elongation machinery remain elusive.[28,36,37]

CH model principles in a single-cell world

While Cooper and Helmstetter make a point of noting that their model applies to idealized average cells, the CH model is frequently applied with the assumption that the average cell and the individual cell are one and the same. Misapplication of this model to single-cell experiments washes out stochastic effects and phenotypic heterogeneity. (**Fig. 2**) In single cells, stochasticity is inherent to both growth rate and the temporal progression of cell cycle events even under so-called "steady-state" conditions.[38–40] Single cell growth rate alone can vary as much as 3-fold under these apparently steady-state conditions. Rather than replication elongation proceeding at a constant rate,[8] single cell data indicate that elongation rate can vary between 250 to 1000 nucleotides/second (nt/s) in individual *E. coli* cells, though most forks proceed at a rate between

550 to 750 nt/s.[41–43] Conflicts between the replisome and transcription machinery,[44–49] genome repair complexes,[50–53] or nucleoid-associated proteins, [54–61] all can influence the instantaneous speed of a given replisome, impacting C period at the single cell level.

Transition to single-cell technology and corresponding modeling advancements

Progressing from the baby machine, early single cell experiments visualized cells grown on a solid surface, typically an agarose pad infused with growth medium.[62–67] These experiments are limited in the total number of generations evaluated, as cells eventually form microcolonies that alter the microenvironment and preclude effective imaging. Advances in microfluidics led to the development of micro-chemostats, such as the mother machine.[40,67–72] The mother machine permits continuous growth over many generations as older cells are swept away from their newborn counterparts by the flow of fresh growth medium.

Importantly, the evaluation of single-cell data requires specific single-cell mathematical parameters. For example, earlier references to MDT refer to the average time required for a cell population to double in mass.[3,73] Typically, the optical density of a culture is measured over time using a spectrophotometer.[74] Then, the slope of the linear range of the log transformed data is used to calculate the MDT. In contrast, the generation time of a given cell cycle of single cells is the time between birth and division of that cell cycle. Measuring this requires precise measurements of the stochastic times at which each individual cell divides and tracking temporal evolution of single cells across multiple movie frames.

With the foundational principles of the CH model as a guide, advances in single-cell technology led to parallel advances in single-cell modeling. In recent years, multiple single-cell models emerged, each designed to address a specific question.[38,40,41,75,76] Generally, the goals of these studies center around understanding how size control is achieved and demystifying the relationship between cell size and replication initiation. At the same time, none of these models take into account single cell data indicating a high degree of stochasticity in the timing and duration of cell cycle events, differences in cell cycle dynamics between wild type and mutant cells, and genetic data hinting at connections between different aspects of cell cycle progression and various steps in central carbon metabolism. [9,28,36,37,77–81] Together, these disconnects suggest the need for a more nuanced and agnostic framework from which to understand the forces governing bacterial cell cycle progression.

An agnostic model of the bacterial cell cycle reliant on stochastic timers

Acknowledging the stochasticity inherent in single cell data and leveraging existing data sets,[40] we developed an agnostic model of the bacterial cell cycle. This model differs from other available models by centering on the idea that at each initiation event, three new stochastic "timers"—corresponding respectively to inter-initiation time, $\boldsymbol{\tau_i}$; fork completion time (C period duration), $\boldsymbol{\tau_C}$; and the time between initiation and the corresponding division event, $\boldsymbol{\tau_d}$—all begin to tick (**Fig. 3**) Thus, the fork number at the start of the next replication cycle is determined by the relative order of completion of these three timers. For a given growth condition, the stochastic distributions of these time periods are functions of the stochastic single-cell exponential growth rate, $\boldsymbol{k}$. Functional dependencies on k can be extracted from published single-cell data.

To test the validity of this model, we leveraged raw data published by the Jun lab, originally generated to study a different question, namely, the validity of the independent double adder model of size control.[40] These data span three growth conditions: M9 acetate (MDT 195 min, equivalent to CH's slow regime), and MOPS glucose and MOPS glycerol 11aa (MDTs 52 min and

63 min, respectively, both near the transition between CH's slow and fast regimes).

We observed that the distributions of all three variables (τ_i, τ_C and τ_d) vary with single-cell growth rate, precluding our ability to simulate these quantities stochastically over consecutive replication cycles. This finding is consistent with previous reports[38–40] indicating that τ_C is generally a function of single-cell growth rate in slow growing populations, but contrary to the deterministic CH model's constant C period (which corresponds to our τ_C) and C+D period (which corresponds to our τ_d).

To overcome this hurdle, we identified emergent simplicities, or scaling collapses and generated calibration curves for each media condition. Briefly, we plotted all data points for each of the three timescales relative to the single-cell exponential growth rate. We then subtracted the best fit mean at the corresponding growth rate from each data point and divided the resulting value by the best fit standard deviation (S.D.) at that growth rate. Finally, we measured the probability distribution

$$P(x|k) = \frac{1}{\sigma_{x|k}} F\left(\frac{x-\langle x|k\rangle}{\sigma_{x|k}}\right) \qquad \textbf{(Eq. 1)}$$

of these scaled values, ***F***.

Within experimental error, the growth rate-independent distribution *F* can be appropriately scaled as shown in **Eq. 1** to give the conditional distribution of the stochastic timescale in question at any given growth rate, with the appropriate mean and variance, and approximate correct shape. Here, x is the stochastic timescale in question; $\sigma_{x|k}$ and $\langle x|k\rangle$ are the fitted S.D. and mean, respectively, as functions of k. (See **Fig. S1 A, B, D, E, G, H**) We performed a similar analysis to characterize the dependence of k during a given inter-initiation cycle on its value during the previous cycle (**Figs. S1C, F, I**). Together, these experiment-derived calibration curves serve as inputs into our initiation-controlled triple timer model. In simulations, we use these input distributions (relative to initiation) to obtain the next τ_i, τ_C, τ_d, and k.

As previously reported, under slow growth conditions (M9 acetate), cells typically initiated and completed a single round of replication (single fork) per cell cycle (2-fork cycle in **Fig. 4**, CH model slow growth regime). Mathematically, the hierarchy between the three timers can be described as $\tau_i > \tau_d > \tau_C$. While single fork replication was the norm, in some cases, after termination we observed a new round of replication initiation prior to division ($\tau_d > \tau_i > \tau_C$), leading to a state with a total of four active replication forks divided across two chromosomes (*ori:ter* = 4:2, **Fig. 4**). Thus, the number of replication forks per cell immediately after initiation depended only on the order of division relative to initiation. Altogether, in slow growth conditions, our model can be simplified to require input of only two timers as functions of k: (i) **inter-initiation time**, τ_i; and (ii) **time to division**, τ_d. Using this streamlined model and the calibration curves obtained from the same single-cell dataset (**Fig. S1**), we simulated the population distribution of the number of replication forks per cell. The results of our fitting parameter-free simulations matched experimental data very well (**Fig. 5A**).

Notably, although population MDTs in MOPS glucose and MOPS glycerol 11aa are on either side of the Cooper-Helmstetter 60-minute MDT transition point between the slow and fast regimes (MDTs 52 min and 63 min respectively), we do not observe an abrupt plateau in C period under either condition. Consistent with a positive relationship between growth rate and initiation frequency, multifork replication is both more prevalent and more complex under the two intermediate growth conditions, MOPS glucose and MOPS glycerol 11aa.[40] We observe both single and multifork replication states among the population (4- and 6-fork cycles, **Fig. 5B, C**). In these conditions, single fork replication is identical to the 4-fork replication of the slow regime ($\tau_d > \tau_i > \tau_C$), while the multifork replication occurs when a new round of replication is initiated prior to completion of the ongoing round of replication, resulting in 6 forks ($\tau_d > \tau_C > \tau_i$). Thus, for these datasets, our model can be simplified to require only τ_i and τ_C to differentiate between

single and multifork replication. As with the slow growth dataset, we measured calibration curves for τ_i, τ_C, and k, then used our framework to simulate the population distribution of the number of replication forks per cell.

Relationship between timers dictates replication fork number

In the CH framework, multifork replication is often viewed as an adaption to the plateau in C period in the fast growth regime.[24] In this view, multifork replication allows mass doubling time to be less than the time required to initiate and complete a new round of replication. While single cell data do not support the existence of two distinct growth regimes, we still observe a clear divergence between single cell growth rate and C-period in fast-growing subpopulations of single-cell datasets, suggesting that τ_C may eventually plateau under more nutrient rich conditions.

Combining the behavior of our model's timers during slow and intermediate growth with the available population-level data for fast growth conditions, we propose that C period gradually flattens as single cell growth rate increases. From an unconstrained mathematical perspective, at the population level, τ_d is expected to plateau as population MDT is reduced, since τ_d is always greater than τ_C, by definition. (**Fig. 3**) In contrast, due to the constraint that every division must be preceded by a corresponding initiation, population-averaged τ_i follows the same trend as doubling time when nutrient imposed growth rate is varied.

Taken together, the measured and predicted timer behaviors suggest that multifork replication is a consequence of changes in the relationship between individual timers at faster single cell growth rates. Timers show differential impacts on the cell cycle depending on growth regime (i.e., slow, intermediate, or fast growth). During slow growth, fork numbers are solely determined by the relative order of τ_i and τ_d, while during intermediate growth they are determined by τ_i and τ_C. During fast growth, we predict that all three timers play a role in determining fork numbers, especially during growth conditions that promote a mixture of allowable chromosome configurations and fork numbers. At the population level, our model predicts the emergence of 8-fork (or more) cycles ($\tau_i<\tau_C<2\tau_i<\tau_d<3\tau_i$) during fast growth, a mixture of 4-fork ($\tau_C<\tau_i< \tau_d<2\tau_i$) and 6-fork cycles ($\tau_i<\tau_C< \tau_d<2\tau_i$) during intermediate growth (near 60 min MDT), and a combination of 2-fork and 4-fork cycles during slow growth. Supporting the validity of our model, we obtained a close match with both experimental data without any fitting parameters (**Fig. 5B, C**), and an updated and more detailed rendering of the CH model (**Fig. 6** vs**. Fig. 1**). Together these results suggest that multifork replication in *E. coli,* at least under slow and intermediate growth conditions, is indeed a consequence of stochastic variation of the three timers (τ_i, τ_C, and τ_d) as a function of single cell growth rate.

A roadmap for the application of this model to open biological questions

While the elegance and simplicity of a thoughtful model can appreciated by physicists and biologists alike, the path from conceptualization to application can be daunting. To clarify this oft-overlooked intermediate step bridging theoretical and applied biophysics, we sought to illuminate the factors underlying the divergence between τ_C and single cell growth rate, a point of agreement between our framework and Cooper and Helmstetter's model.

There are three possible explanations for the divergence of τ_C and the plateau in population average C-period in fast growing cells. First, as has been suggested, DNA polymerase simply reaches maximum velocity.[8] We do not favor this idea based on population data indicating that C-period is reduced as much as 30% in short *E. coli* mutants and *E. coli* cells in which levels of the initiator protein, DnaA, are reduced delaying the onset of replication.[28] In other words, if there

are circumstances in which the replisome can more faster, it will. Of possible alternative explanations, two seem most likely given the positive association between reductions in replisome efficiency and multifork replication: titration of limiting replication substrates or enzymes ("titration model," **Fig. 7A**), and physical constraints of fork spacing ("fork spacing model," **Fig. 7B**). Importantly, both proposed mechanisms are expected to alter replication kinetics in a growth rate-dependent manner. In the titration model, replisome protein copy number and dNTP concentration are both expected to correlate with growth rate. In the fork spacing model, both transcription-dependent supercoiling and DNA crowding are also expected to correlate with growth rate.

With our approach, we can measure τ_i and τ_C, but also fork number, which uniquely positions us to distinguish between these scenarios. A reduction in τ_i and τ_C (and consequently τ_d) relative to k in a fast-growing population that is *independent* of total fork number would be consistent with titration of a limiting reagent under these conditions. Conversely, reductions in τ_i and τ_C that are *correlated* with fork number would support a fork-spacing model due to the increased number of replication forks progressing on a single strand.

Applying this "test" we find that in both growth media in which multifork replication is prevalent, (MOPS Glucose, MDT 52 min; MOPS Glycerol + 11 amino acids, MDT 64 min),[40] we observe diminishing returns to replication rate on increasing k, *independent* of the number of replication forks present (**Fig. 8**) in individual cells. While larger data sets representing a wider range of growth conditions will be required for confirmation, so far, this finding argues against a model in which individual replication forks on the same chromosomal arm interfere with one another. Instead, it suggests that titration of essential substrates or polymerase components is the most likely explanation for diminishing returns to replisome speed in rapidly growing single cells.

Discussion

Scientific progress depends on our ability to incorporate new information, and is often driven by technological advancement. Just as the CH model was born out of the baby machine invention, a new model is required to capture the vast information provided by single-cell microfluidics experiments. While the CH model has served a valuable function—contextualizing and inspiring work on the bacterial cell cycle for over 50 years—rapid advances in single cell analysis reveal its limitations.

To fill this gap, we developed new framework with which to understand cell cycle coordination. Our model accounts for the stochasticity, an intrinsic and ubiquitous phenomenon at the single cell level that is washed out in population based data sets. (**Fig. 2**) In contrast to the CH model, in which multifork replication was viewed as an adaptation to a plateau in C-period in fast growing cells, our model suggests it is a consquence of multiple factors including stochasticity in the timing of key cell cycle events—motivating an explanation for its presence in subsets of slow growing cells, and divergence between τ_C and single cell growth rate in fast growing populations. Notably, when our model's timers are mapped to the population level, the resulting picture suggests that C period *gradually* tapers to its minimum value as average growth rate increases with increases in nutrient availability. This view is in distinct contrast to the sharp plateau in C period that distinguishes Cooper and Helmstetter's fast growth and slow growth regimes.

This framework offers numerous advantages for the evaluation of single-cell data. Importantly, our model may be applied to any strain in any growth medium in any growth regime. Our model is agnostic to the mechanism underlying the stochastic dynamics of initiation, replication and division, and simply captures these dynamics through the experimentally measured "calibration curves" for each of these timers as functions of single cell growth rate. Many population studies apply equations rooted in wildtype deterministic models to mutant strain populations which may

result in misleading or inaccurate conclusions. Ultimately, the flexibility confered by these calibration curves uniquely positions our model to answer unaddressed questions about the impacts of mutations and nutrient composition on the bacterial cell cycle and its regulation.

In an effort to demystify the process of applying mathematical models to biological questions, we compared single-cell behavior to identify titration of key substrates and/or replisome components as the most likely cause of diminishing returns on C period at faster single cell growth rates (**Fig. 8, Fig. S1**). Despite the seemingly abundant levels of replisome enzymes and its dNTP substrates, slight changes in transcript and protein production relative to growth rate could easily skew reaction kinetics such that local concentrations of one or more components at the replisome drops to either subsaturating or sub-Km levels. In many ways, the titration model encompasses the idea of a maximum replisome velocity, but this maximum velocity is dependent on environmental and nutrient conditions. Thus, titration of substrates and/or components may underlie differences in calibration curves between media with relatively similar growth rates (**Fig. S1**). Variations in nutrient compositions of two growth media could intrinsically shift metabolic flux to or from the pathways required for producing enzyme or substrate precursors. This titration model idea also aligns with the idea of a general growth law, which is based on the principle of a "unit cell" containing the minimal resources for self-duplication.[25] SS and PAL are currently screening a library of *E. coli* mutants to identify metabolic nodes impacting various aspects DNA replication, to clarify the relationship between nutrient availability and this essential aspect of cell cycle regulation. (*manuscript in preparation*)

In sum, recognizing the value of single cell data as a framework from which to understand the molecular mechanisms underlying cell cycle progression in bacterial cells is just the first step. Larger, more comprehensive single cell data sets spanning a wide range of MDTs and media compositions is essential to determine the relationship between nutrient availability and cell cycle progression at high resolution. This type of data will clarify the impact of media composition on DNA replication, resolve outstanding questions about the validity of the CH model's two regime framwork, particularly with regard to the plateau in C period at MDT < 60 minutes, and illuminate the mechanisms underlying the relationship between replication fork number and elongation rate in fast growing cells. Looking ahead, it will also be important to apply our stochastic framework to mutants that traditional methods indicate exhibit reductions in C-period length[28,82] to determine if τ_C is indeed faster in individual cells. Our stochastic framework will also be useful in the study of organisms like *B. subtilis,* which do not appear to coordinate the initiation of replication with achievement of a specific size[28] and *Mycobacteria,* which reportedly does not undergo multifork replication (except infrequent cases that may be explained by stochasticity).[83,84] We look forward to the next chapter!

Author Contributions

P.A.L. and S.I.-B. conceived of and designed research; S.S. and K.J. analyzed the extant data; S.S. spearheaded the writing process, contextualized the existing literature, and conceptually integrated biological and biophysical findings; K.J. formulated the model, analyzed the single-cell datasets, and performed analytic calculations and simulations under the guidance of S.I.-B.; all authors discussed the results and wrote the paper.

Acknowledgements

We thank Suckjoon Jun and Fangwei Si for generously sharing the details of their methodology and analysis, along with the raw, single-cell data sets that are the heart of this study.[40] We also thank them for in-depth discussions of the implications inherent in their approach. We are grateful

to the Levin and Iyer-Biswas groups for their insights and input as we pressure tested multiple iterations of the model and its implications. P.A.L. and S.I.-B. thank the Aspen Center for Physics for graciously hosting us, and making our collaboration possible.

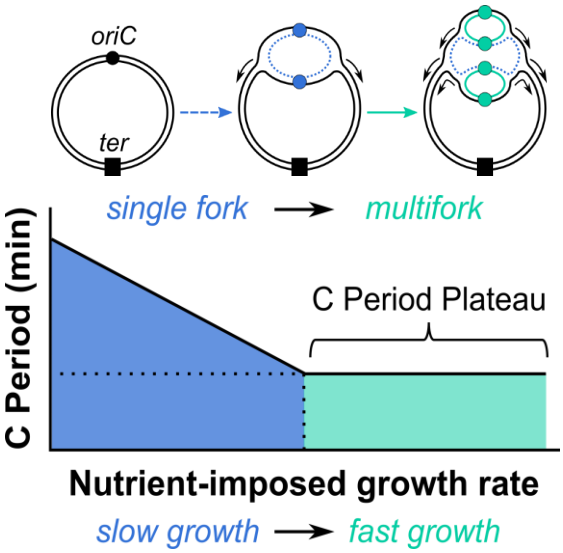

Fig. 1. Replication of the *E. coli* chromosome. *Top:* Bacterial chromosome depicting the origin of replication (*oriC,* ●) and terminus *(ter*, ■). After birth, replication initiation yields a single replication bubble, a replication state termed "single fork replication" (---). When a second initiation event occurs before termination of the prior round, "multifork replication" occurs (—). Active origins and newly synthesized DNA are indicated with colors corresponding to replication state. *Bottom:* In the Cooper-Helmstetter model, as nutrient-imposed growth rate increases, the C period length decreases until it reaches a plateau during fast growth**.**

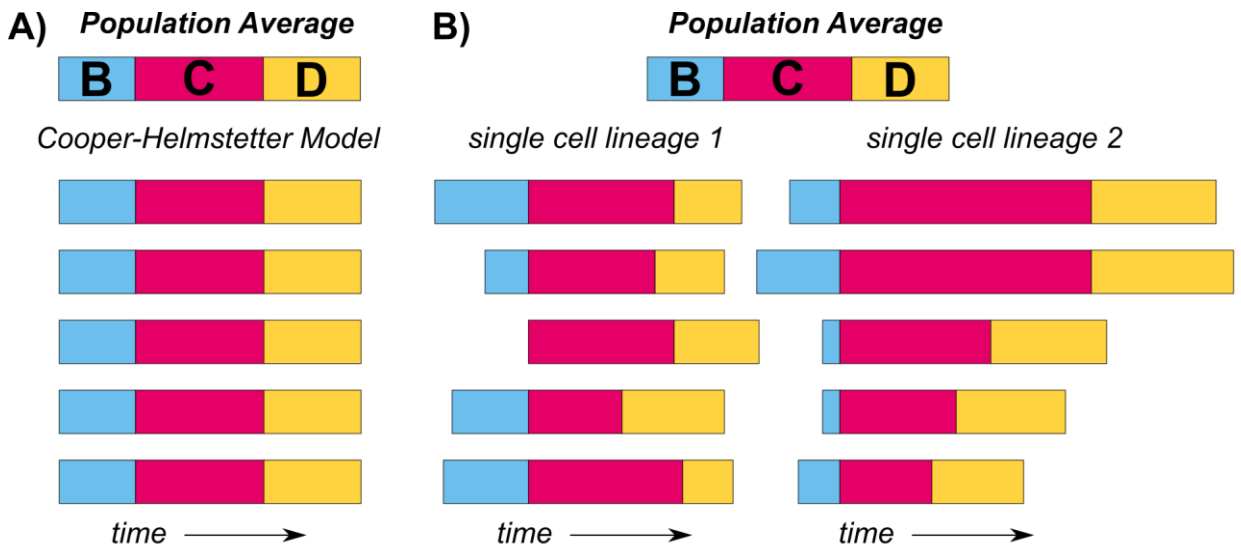

Fig. 2. Deterministic paradigm vs. stochastic nature of cell cycle timescales. (A) The CH model assumes that all cells within a given condition follow the population average B, C, and D periods. (B) ~~Actual~~ Relative B, C, and D periods are shown over multiple consecutive replication cycles for two cell lineages grown on MOPS glucose (based on data from Si et al.). Significant differences between replication cycles necessitate a new theory

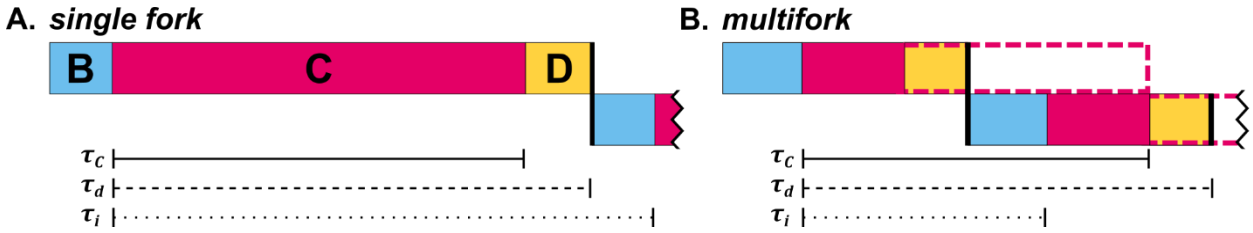

Fig. 3: Stochastic Timers. Visual representations of the timers τ_i, τ_C and τ_d in a cell undergoing single fork (A) and multifork (B) replication. During multifork replication, C periods extend beyond a single division cycle. This overlap is indicated by extended dotted lines. Color schemes match Fig. 2.

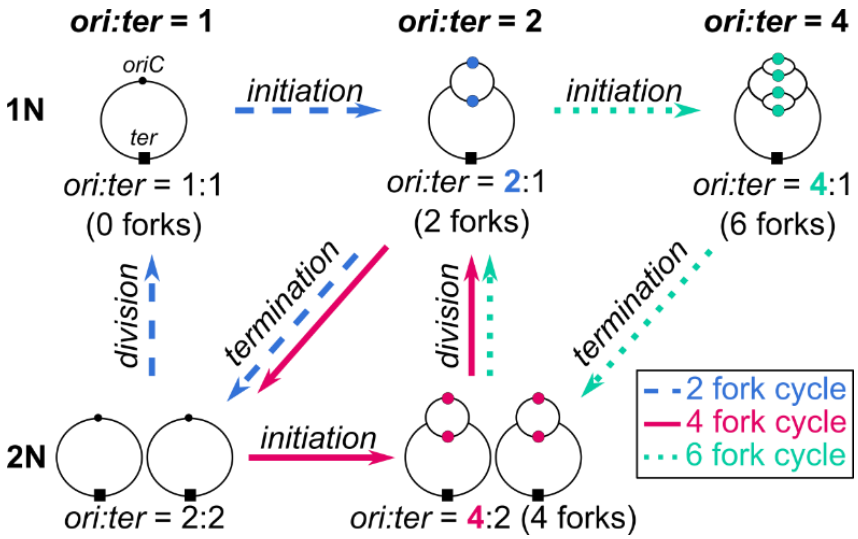

Fig. 4: Flow chart depicting the possible replication cycles depending on the order of initiation, termination, and division events. *N* represents the number of chromosome copies present in the cell and is equal to the number of termini (*ter*, ■). 2-fork cycle (blue) forms two forks upon initiation at *oriC*, ●, then replication is completed leaving zero forks. 4-fork cycle (magenta) progresses from 4 forks at initiation to 2 forks after division to termination. 6-fork cycle (teal) progresses from 6 forks at initiation to 4 forks after termination of previous replication to 2 forks after division to 6 forks after new round of initiation. Further configurations with 8 forks or more are relevant only at growth rates faster than available in this dataset.

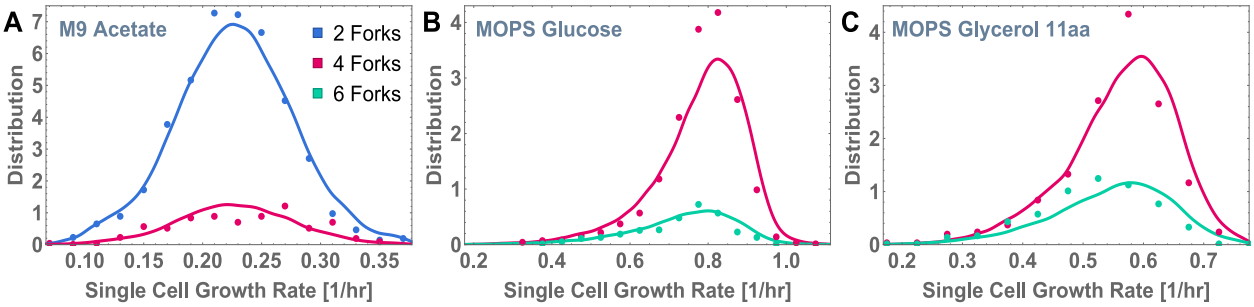

Fig. 5: Comparing model predictions to experimental data. Model simulations (dashed lines) are compared with the experimentally obtained distributions (solid lines) of number of forks after initiation at different single cell growth rates for the following growth conditions: (A) M9 acetate, (B) MOPS glucose and (C) MOPS glycerol 11aa. Colors represent different number of forks after initiation: 2 (blue), 4 (magenta), and 6 (teal). There is a close match between model predictions and experimental data, indicating that the presence of different numbers of forks and both single and multifork replication within the same growth condition is purely a consequence of the inherent stochasticity in the three time periods governing the replication cycle (the C period, the inter-initiation period, and the time to division), each of which depends solely on single-cell growth rate for a given growth condition.

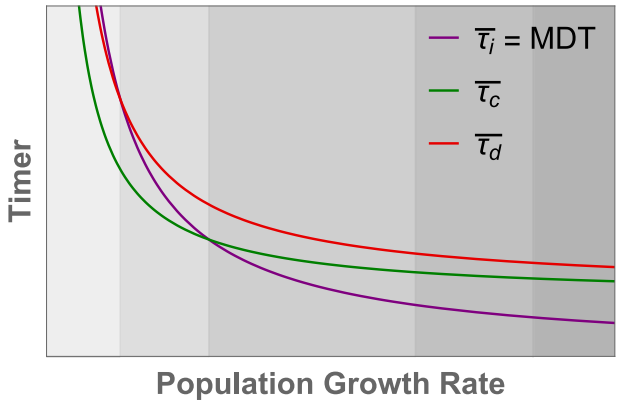

Forks	Order
2	$\overline{\tau_c}<\overline{\tau_d}<\overline{\tau_i}$
4	$\overline{\tau_c}<\overline{\tau_i}<\overline{\tau_d}<2\overline{\tau_i}$
6	$\overline{\tau_i}<\overline{\tau_c}<\overline{\tau_d}<2\overline{\tau_i}$
8	$\overline{\tau_i}<\overline{\tau_c}<2\overline{\tau_i}<\overline{\tau_d}<3\overline{\tau_i}$
14	$2\overline{\tau_i}<\overline{\tau_c}<\overline{\tau_d}<3\overline{\tau_i}$

Fig. 6: Determining fork numbers from nutrient-imposed population growth rate. Our expectation for the trends in population mean values of τ_i, τ_C, and τ_d as a function of nutrient-imposed population growth rate. We expect mean τ_C and τ_d to flatten as growth rate goes to infinity, while mean τ_i (equal to MDT) approaches zero. Fork numbers at different population growth rates are determined by the relative order of these timers, as shown.

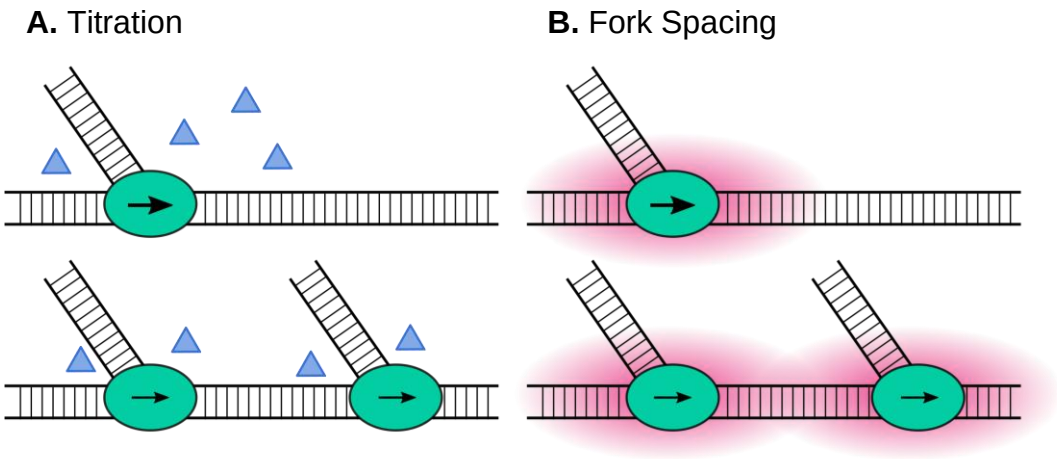

Fig. 7: Two hypothesized models for C period decrease as growth rate increases. A) titration. B) fork spacing. Ovals represent active replisomes, triangles represent accessory replisome components and dNTP substrates, arrows represent relative replisome speed, and red clouds around the replisome represent steric repulsion and topological changes that alter replisome kinetics.

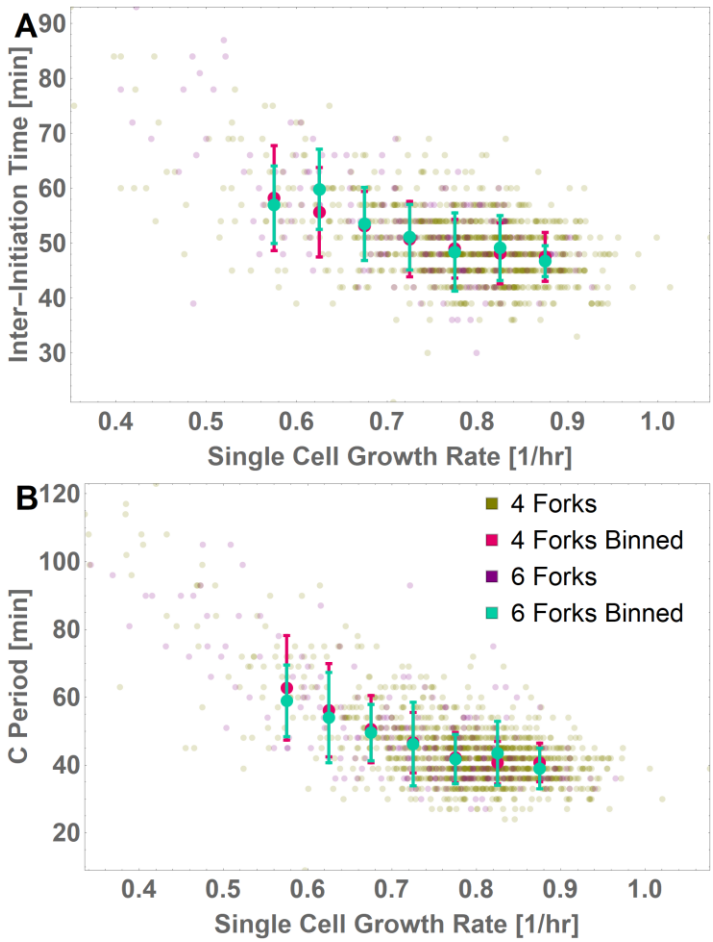

Fig. 8: Both Inter-initiation time and C period are independent of fork number. (A) Inter-initiation time (τ_i) and (B) C period (τ_C) is plotted against single cell growth rate (k) for an intermediate growth condition (medium 4). Mean and S.D. of binned C periods and the spread of data points are plotted separately for ● 4-fork (single fork) and ● 6-fork (multifork) data, based on the fork number observed just after initiation.

Supplemental Information

Fig. S1. Calibration curves used as inputs in the model. For cells growing in (A-C) M9 Acetate, (D-F) MOPS Glucose, and (G-I) MOPS Glycerol 11aa, data points with binned mean and S.D. of (A, D, G) inter-initiation time, (B) Time to Division in slow growth condition (as explained in the main text, intermediate growth conditions require C Period instead, which are plotted in (E, H)), and (C, F, I) single-cell growth rate of subsequent generation are plotted as a function of single-cell growth rate of current generation (inset: S.D. as a function of growth rate for the corresponding binned points). The orange line is the best fit line (A and B: y=a+b/x and C: y=a+bx) fit using the binned mean. The observation that each binned mean and S.D. are quantitatively related enables us to use Eq. 1 to represent the different distributions at different single-cell growth rates within a growth condition by the same invariant rescaled distribution. This results in a significant simplification of model complexity. Orange best fit curves correspond to the mean and S.D. of these quantities, which we take as inputs to our model when using the rescaled distribution formulation; thus, their match with the green binned experimental data points is essential for accuracy of our results. Note that the S.D. in (C) inset for M9 Acetate is almost constant (with a variation of only 8%).

M9 Acetate:

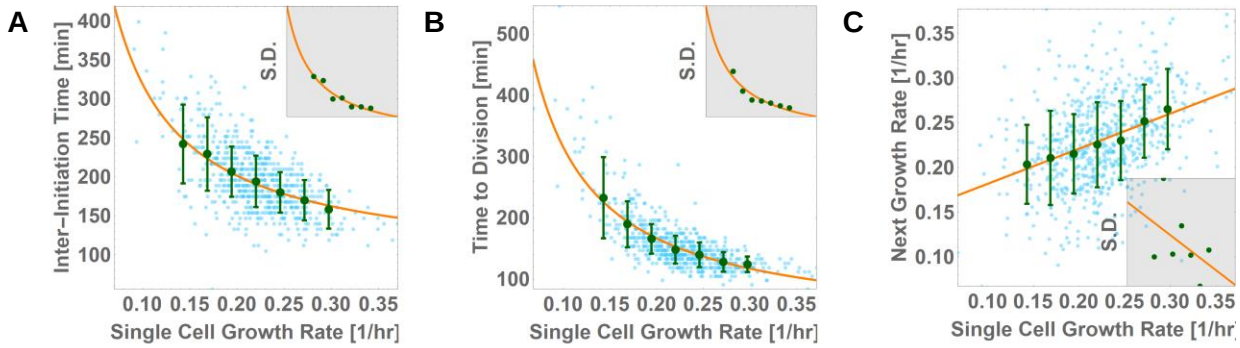

MOPS Glucose

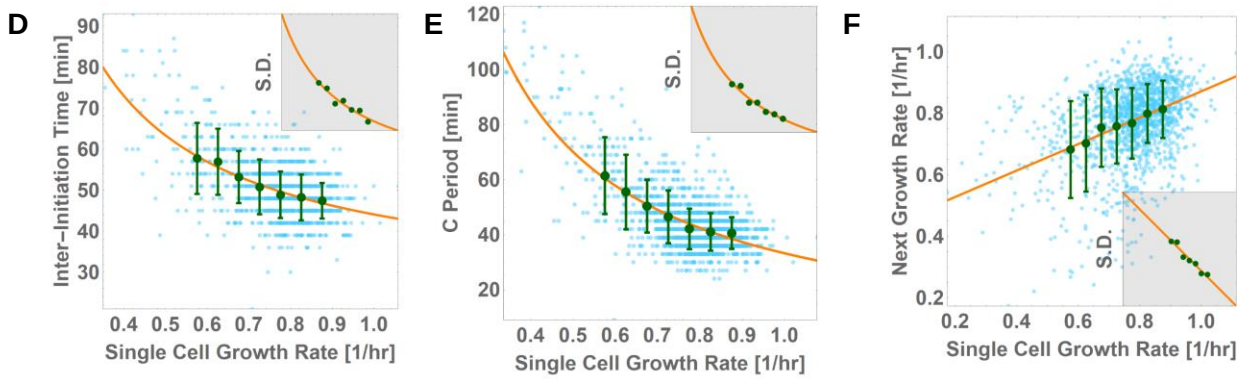

MOPS Glycerol 11aa:

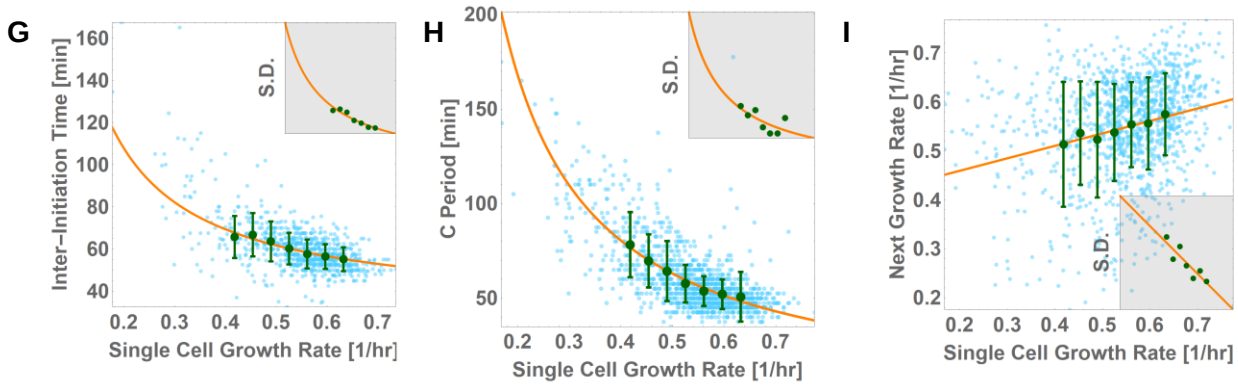

References

1. Cooper G. *The Cell: A Molecular Approach*. 2nd edition. Sinauer Associates; 2000. Accessed June 24, 2021. https://www.ncbi.nlm.nih.gov/books/NBK9876/

2. Vadia S, Tse JL, Lucena R, et al. Fatty Acid Availability Sets Cell Envelope Capacity and Dictates Microbial Cell Size. *Curr Biol CB*. 2017;27(12):1757-1767.e5. doi:S0960-9822(17)30642-5

3. Schaechter M, Maaløe O, Kjeldgaard NO. Dependency on medium and temperature of cell size and chemical composition during balanced grown of *Salmonella typhimurium*. *J Gen Microbiol*. 1958;19(3):592-606. doi:10.1099/00221287-19-3-592

4. Pierucci O. Dimensions of *Escherichia coli* at various growth rates: model for envelope growth. *J Bacteriol*. 1978;135(2):559-574. doi:10.1128/jb.135.2.559-574.1978

5. Levin PA, Janakiraman A. Localization, Assembly, and Activation of the *Escherichia coli* Cell Division Machinery. *EcoSal Plus*. 2021;9(2):eESP00222021. doi:10.1128/ecosalplus.ESP-0022-2021

6. Wu LJ, Errington J. Coordination of cell division and chromosome segregation by a nucleoid occlusion protein in *Bacillus subtilis*. *Cell*. 2004;117(7):915-925. doi:10.1016/j.cell.2004.06.002

7. Bernhardt TG, de Boer PAJ. SlmA, a nucleoid-associated, FtsZ binding protein required for blocking septal ring assembly over chromosomes in *E. coli*. *Mol Cell*. 2005;18(5):555-564. doi:10.1016/j.molcel.2005.04.012

8. Cooper S, Helmstetter CE. Chromosome replication and the division cycle of *Escherichia coli* B/r. *J Mol Biol*. 1968;31(3):519-540. doi:10.1016/0022-2836(68)90425-7

9. Wang JD, Levin PA. Metabolism, cell growth and the bacterial cell cycle. *Nat Rev*. 2009;7(11):822-827. doi:10.1038/nrmicro2202

10. Cairns J. The bacterial chromosome and its manner of replication as seen by autoradiography. *J Mol Biol*. 1963;6:208-213. doi:10.1016/s0022-2836(63)80070-4

11. Schaechter M, Bentzon MW, Maaløe O. Synthesis of Deoxyribonucleic Acid during the Division Cycle of Bacteria. *Nature*. 1959;183(4669):1207-1208. doi:10.1038/1831207a0

12. Pachler PF, Koch AL, Schaechter M. Continuity of DNA synthesis in *Escherichia coli*. *J Mol Biol*. 1965;11(3):650-653. doi:10.1016/S0022-2836(65)80020-1

13. Lark KG, Maaløe O. Nucleic acid synthesis and the division cycle of *Salmonella typhimurium*. *Biochim Biophys Acta*. 1956;21(3):448-458. doi:10.1016/0006-3002(56)90181-0

14. Vadia S, Levin PA. Growth rate and cell size: a re-examination of the growth law. *Curr Opin Microbiol*. 2015;24:96-103. doi:10.1016/j.mib.2015.01.011

15. Sauls JT, Cox SE, Do Q, Castillo V, Ghulam-Jelani Z, Jun S. Control of *Bacillus subtilis* Replication Initiation during Physiological Transitions and Perturbations. *mBio*. 2019;10(6). doi:10.1128/mBio.02205-19

16. Helmstetter CE. DNA synthesis during the division cycle of rapidly growing *Escherichia coli* B/r. *J Mol Biol*. 1968;31(3):507-518. doi:10.1016/0022-2836(68)90424-5

17. Donachie WD. Relationship between cell size and time of initiation of DNA replication. *Nature*. 1968;219(5158):1077-1079. doi:10.1038/2191077a0

18. Jameson KH, Wilkinson AJ. Control of Initiation of DNA Replication in *Bacillus subtilis* and *Escherichia coli*. *Genes*. 2017;8(1):10.3390/genes8010022

19. Wold S, Skarstad K, Steen HB, Stokke T, Boye E. The initiation mass for DNA replication in *Escherichia coli* K-12 is dependent on growth rate. *EMBO J*. 1994;13(9):2097-2102.

20. Zheng H, Bai Y, Jiang M, et al. General quantitative relations linking cell growth and the cell cycle in *Escherichia coli*. *Nat Microbiol*. 2020;5(8):995-1001. doi:10.1038/s41564-020-0717-x

21. Churchward G, Estiva E, Bremer H. Growth rate-dependent control of chromosome replication initiation in *Escherichia coli*. *J Bacteriol*. 1981;145(3):1232.

22. Micali G, Grilli J, Marchi J, Osella M, Cosentino Lagomarsino M. Dissecting the Control Mechanisms for DNA Replication and Cell Division in *E. coli*. *Cell Rep*. 2018;25(3):761-771.e4. doi:10.1016/j.celrep.2018.09.061

23. Micali G, Grilli J, Osella M, Lagomarsino MC. Concurrent processes set *E. coli* cell division. *Sci Adv*. 2018;4(11). doi:10.1126/sciadv.aau3324

24. Jun S, Si F, Pugatch R, Scott M. Fundamental Principles in Bacterial Physiology - History, Recent progress, and the Future with Focus on Cell Size Control: A Review. *Rep Prog Phys Phys Soc G B*. 2018;81(5):056601. doi:10.1088/1361-6633/aaa628

25. Si F, Li D, Cox SE, et al. Invariance of Initiation Mass and Predictability of Cell Size in *Escherichia coli*. *Curr Biol CB*. 2017;27(9):1278-1287. doi:S0960-9822(17)30291-9

26. Løbner-Olesen A, Skarstad K, Hansen FG, von Meyenburg K, Boye E. The DnaA protein determines the initiation mass of *Escherichia coli* K-12. *Cell*. 1989;57(5):881-889. doi:10.1016/0092-8674(89)90802-7

27. Grant MA, Saggioro C, Ferrari U, Bassetti B, Sclavi B, Cosentino Lagomarsino M. DnaA and the timing of chromosome replication in *Escherichia coli* as a function of growth rate. *BMC Syst Biol*. 2011;5(1):201. doi:10.1186/1752-0509-5-201

28. Hill NS, Kadoya R, Chattoraj DK, Levin PA. Cell size and the initiation of DNA replication in bacteria. *PLoS Genet*. 2012;8(3):e1002549. doi:10.1371/journal.pgen.1002549

29. Grimwade JE, Rozgaja TA, Gupta R, Dyson K, Rao P, Leonard AC. Origin recognition is the predominant role for DnaA-ATP in initiation of chromosome replication. *Nucleic Acids Res*. 2018;46(12):6140-6151. doi:10.1093/nar/gky457

30. Fingland NK. Acidic phospholipid deficiency results in an inhibition of chromosomal replication and cell-cycle specific arrest in *Escherichia coli*. Published online January 1, 2012. https://search.proquest.com/docview/926210655

31. Magnan D, Bates D. Regulation of DNA Replication Initiation by Chromosome Structure. *J Bacteriol*. 2015;197(21):3370-3377. doi:10.1128/JB.00446-15

32. Katayama T. Initiation of DNA Replication at the Chromosomal Origin of *E. coli*, *oriC*. In: Masai H, Foiani M, eds. DNA Replication: From Old Principles to New Discoveries. Springer Singapore; 2017:79-98. doi:10.1007/978-981-10-6955-0_4

33. Katayama T, Kasho K, Kawakami H. The DnaA Cycle in *Escherichia coli*: Activation, Function and Inactivation of the Initiator Protein. *Front Microbiol*. 2017;8. doi:10.3389/fmicb.2017.02496

34. Ho PY, Amir A. Simultaneous regulation of cell size and chromosome replication in bacteria. *Front Microbiol*. 2015;6. Accessed March 13, 2022. https://www.frontiersin.org/article/10.3389/fmicb.2015.00662

35. Wang JD, Sanders GM, Grossman AD. Nutritional control of elongation of DNA replication by (p)ppGpp. *Cell*. 2007;128(5):865-875. doi:S0092-8674(07)00130-4

36. Guarino E, Jiménez-Sánchez A, Guzmán EC. Defective ribonucleoside diphosphate reductase impairs replication fork progression in *Escherichia coli*. *J Bacteriol*. 2007;189(9):3496-3501. doi:10.1128/JB.01632-06

37. Moreno SG, Martín CM, Guillén EF, Guzmán EC. Tuning the replication fork progression by the initiation frequency. *Environ Microbiol*. 2013;15(12):3240-3251. doi:10.1111/1462-2920.12127

38. Wallden M, Fange D, Lundius EG, Baltekin Ö, Elf J. The Synchronization of Replication and Division Cycles in Individual *E. coli* Cells. *Cell*. 2016;166(3):729-739. doi:10.1016/j.cell.2016.06.052

39. Adiciptaningrum A, Osella M, Moolman MC, Cosentino Lagomarsino M, Tans SJ. Stochasticity and homeostasis in the *E. coli* replication and division cycle. *Sci Rep*. 2015;5:18261. doi:10.1038/srep18261

40. Si F, Treut GL, Sauls JT, Vadia S, Levin PA, Jun S. Mechanistic Origin of Cell-Size Control and Homeostasis in Bacteria. *Curr Biol CB*. 2019;29(11):1760-1770.e7. doi:10.1016/j.cub.2019.04.062

41. Pham TM, Tan KW, Sakumura Y, Okumura K, Maki H, Akiyama MT. A single-molecule approach to DNA replication in *Escherichia coli* cells demonstrated that DNA polymerase III is a major determinant of fork speed. *Mol Microbiol*. 2013;90(3):584-596. doi:10.1111/mmi.12386

42. Bhat D, Hauf S, Plessy C, Yokobayashi Y, Pigolotti S. Speed fluctuations of bacterial replisomes. Published online December 6, 2021:2021.10.15.464478. doi:10.1101/2021.10.15.464478

43. Graham JE, Marians KJ, Kowalczykowski SC. Independent and Stochastic Action of DNA Polymerases in the Replisome. *Cell*. 2017;169(7):1201-1213.e17. doi:S0092-8674(17)30634-7

44. Wang JD, Berkmen MB, Grossman AD. Genome-wide co-orientation of replication and transcription reduces adverse effects on replication in *Bacillus subtilis*. *Proc Natl Acad Sci*. 2007;104(13):5608-5613. doi:10.1073/pnas.0608999104

45. Syeda AH, Dimude JU, Skovgaard O, Rudolph CJ. Too Much of a Good Thing: How Ectopic DNA Replication Affects Bacterial Replication Dynamics. *Front Microbiol*. 2020;11. doi:10.3389/fmicb.2020.00534

46. Poveda AM, Clech ML, Pasero P. Transcription and replication: Breaking the rules of the road causes genomic instability. *Transcription*. 2010;1(2):99. doi:10.4161/trns.1.2.12665

47. Brüning JG, Marians KJ. Replisome bypass of transcription complexes and R-loops. *Nucleic Acids Res*. 2020;48(18):10353. doi:10.1093/nar/gkaa741

48. Khan SR, Mahaseth T, Kouzminova EA, Cronan GE, Kuzminov A. Static and Dynamic Factors Limit Chromosomal Replication Complexity in *Escherichia coli*, Avoiding Dangers of Runaway Overreplication. *Genetics*. 2016;202(3):945-960. doi:10.1534/genetics.115.184697

49. Cooper DL, Harada T, Tamazi S, Ferrazzoli AE, Lovett ST. The Role of Replication Clamp-Loader Protein HolC of *Escherichia coli* in Overcoming Replication/Transcription Conflicts. *mBio*. 2021;12(2). doi:10.1128/mBio.00184-21

50. Romero ZJ, Chen SH, Armstrong T, et al. Resolving Toxic DNA repair intermediates in every *E. coli* replication cycle: critical roles for RecG, Uup and RadD. *Nucleic Acids Res*. 2020;48(15):8445-8460. doi:10.1093/nar/gkaa579

51. Moolenaar GF, Moorman C, Goosen N. Role of the *Escherichia coli* Nucleotide Excision Repair Proteins in DNA Replication. *J Bacteriol*. 2000;182(20):5706-5714. doi:10.1128/JB.182.20.5706-5714.2000

52. Kuzminov A. Recombinational Repair of DNA Damage in *Escherichia coli* and Bacteriophage λ. *Microbiol Mol Biol Rev*. 1999;63(4):751.

53. Wendel BM, Courcelle CT, Courcelle J. Completion of DNA replication in *Escherichia coli*. *Proc Natl Acad Sci U S A*. 2014;111(46):16454. doi:10.1073/pnas.1415025111

54. Replication fork passage drives asymmetric dynamics of a critical nucleoid-associated protein in *Caulobacter*. *EMBO J*. 2017;36(3):301-318. doi:10.15252/embj.201695513

55. Marczynski GT, Petit K, Patel P. Crosstalk Regulation Between Bacterial Chromosome Replication and Chromosome Partitioning. *Front Microbiol*. 2019;10. doi:10.3389/fmicb.2019.00279

56. Taylor JA, Panis G, Viollier PH, Marczynski GT. A novel nucleoid-associated protein coordinates chromosome replication and chromosome partition. *Nucleic Acids Res*. 2017;45(15):8916. doi:10.1093/nar/gkx596

57. Guo MS, Haakonsen DL, Zeng W, Schumacher MA, Laub MT. A bacterial chromosome structuring protein binds overtwisted DNA to stimulate type II topoisomerases and enable DNA replication. *Cell*. 2018;175(2):583. doi:10.1016/j.cell.2018.08.029

58. Ryan VT, Grimwade JE, Camara JE, Crooke E, Leonard AC. *Escherichia coli* prereplication complex assembly is regulated by dynamic interplay among Fis, IHF and DnaA. *Mol Microbiol*. 2004;51(5):1347-1359. doi:10.1046/j.1365-2958.2003.03906.x

59. Chodavarapu S, Felczak MM, Yaniv JR, Kaguni JM. *Escherichia coli* DnaA interacts with HU in initiation at the E. coli replication origin. *Mol Microbiol*. 2008;67(4):781-792. doi:10.1111/j.1365-2958.2007.06094.x

60. Travers A, Muskhelishvili G. Bacterial chromatin. *Curr Opin Genet Dev*. 2005;15(5):507-514. doi:10.1016/j.gde.2005.08.006

61. Joshi MC, Magnan D, Montminy TP, Lies M, Stepankiw N, Bates D. Regulation of Sister Chromosome Cohesion by the Replication Fork Tracking Protein SeqA. *PLOS Genet*. 2013;9(8):e1003673. doi:10.1371/journal.pgen.1003673

62. Mueller EA, Egan AJ, Breukink E, Vollmer W, Levin PA. Plasticity of *Escherichia coli* cell wall metabolism promotes fitness and antibiotic resistance across environmental conditions. Laub MT, Storz G, Laub MT, eds. *eLife*. 2019;8:e40754. doi:10.7554/eLife.40754

63. Mueller EA, Westfall CS, Levin PA. pH-dependent activation of cytokinesis modulates *Escherichia coli* cell size. *PLOS Genet*. 2020;16(3):e1008685. doi:10.1371/journal.pgen.1008685

64. Rosenfeld N, Young JW, Alon U, Swain PS, Elowitz MB. Gene regulation at the single-cell level. *Science*. 2005;307(5717):1962-1965. doi:10.1126/science.1106914

65. Dunlop MJ, Cox RS, Levine JH, Murray RM, Elowitz MB. Regulatory activity revealed by dynamic correlations in gene expression noise. *Nat Genet*. 2008;40(12):1493-1498. doi:10.1038/ng.281

66. Westfall CS, Levin PA. Comprehensive analysis of central carbon metabolism illuminates connections between nutrient availability, growth rate, and cell morphology in *Escherichia coli*. *PLoS Genet*. 2018;14(2):e1007205. doi:10.1371/journal.pgen.1007205

67. Cabeen MT, Losick R. Single-cell Microfluidic Analysis of *Bacillus subtilis*. *JoVE J Vis Exp*. 2018;(131):e56901. doi:10.3791/56901

68. Bakshi S, Leoncini E, Baker C, Cañas-Duarte SJ, Okumus B, Paulsson J. Tracking bacterial lineages in complex and dynamic environments with applications for growth control and persistence. *Nat Microbiol*. 2021;6(6):783-791. doi:10.1038/s41564-021-00900-4

69. Santi I, Dhar N, Bousbaine D, Wakamoto Y, McKinney JD. Single-cell dynamics of the chromosome replication and cell division cycles in *Mycobacteria*. *Nat Commun*. 2013;4:2470. doi:10.1038/ncomms3470

70. Witz G, van Nimwegen E, Julou T. Initiation of chromosome replication controls both division and replication cycles in *E. coli* through a double-adder mechanism. Laub MT, Storz G, Leonard A, eds. *eLife*. 2019;8:e48063. doi:10.7554/eLife.48063

71. Lambert G, Kussell E. Memory and Fitness Optimization of Bacteria under Fluctuating Environments. *PLOS Genet*. 2014;10(9):e1004556. doi:10.1371/journal.pgen.1004556

72. Salman H, Brenner N, Tung C kuan, et al. Universal Protein Fluctuations in Populations of Microorganisms. *Phys Rev Lett*. 2012;108(23):238105. doi:10.1103/PhysRevLett.108.238105

73. Schaechter M, Williamson JP, Jr JRH, Koch AL. Growth, cell and nuclear divisions in some bacteria. *J Gen Microbiol*. 1962;29:421-434. doi:10.1099/00221287-29-3-421

74. Monod J. The Growth of Bacterial Cultures. *Annu Rev Microbiol*. 1949;3(1):371-394. doi:10.1146/annurev.mi.03.100149.002103

75. Taheri-Araghi S, Bradde S, Sauls JT, et al. Cell-Size Control and Homeostasis in Bacteria. *Curr Biol CB*. 2017;27(9):1392. doi:10.1016/j.cub.2017.04.028

76. Campos M, Surovtsev IV, Kato S, et al. A constant size extension drives bacterial cell size homeostasis. *Cell*. 2014;159(6):1433-1446. doi:10.1016/j.cell.2014.11.022

77. Nouri H, Monnier AF, Fossum-Raunehaug S, et al. Multiple links connect central carbon metabolism to DNA replication initiation and elongation in *Bacillus subtilis*. *DNA Res*. 2018;25(6):641-653. doi:10.1093/dnares/dsy031

78. Tymecka-Mulik J, Boss L, Maciąg-Dorszyńska M, et al. Suppression of the *Escherichia coli dnaA46* mutation by changes in the activities of the pyruvate-acetate node links DNA replication regulation to central carbon metabolism. *PLOS ONE*. 2017;12(4):e0176050. doi:10.1371/journal.pone.0176050

79. Maciąg M, Nowicki D, Janniere L, Szalewska-Pałasz A, Węgrzyn G. Genetic response to metabolic fluctuations: correlation between central carbon metabolism and DNA replication in *Escherichia coli*. *Microb Cell Factories*. 2011;10:19-19. doi:10.1186/1475-2859-10-19

80. Maciąg M, Nowicki D, Szalewska-Pałasz A, Węgrzyn G. Central carbon metabolism influences fidelity of DNA replication in *Escherichia coli*. *Mutat Res*. 2012;731(1-2):99-106. doi:10.1016/j.mrfmmm.2011.12.005

81. Krause K, Maciąg-Dorszyńska M, Wosinski A, et al. The Role of Metabolites in the Link between DNA Replication and Central Carbon Metabolism in *Escherichia coli*. *Genes*. 2020;11(4). doi:10.3390/genes11040447

82. Zhu M, Dai X, Guo W, et al. Manipulating the Bacterial Cell Cycle and Cell Size by Titrating the Expression of Ribonucleotide Reductase. *mBio*. 2017;8(6):1741. doi:10.1128/mBio.01741-17

83. Trojanowski D, Hołówka J, Ginda K, Jakimowicz D, Zakrzewska-Czerwińska J. Multifork chromosome replication in slow-growing bacteria. *Sci Rep*. 2017;7. doi:10.1038/srep43836

84. Logsdon MM, Aldridge BB. Stable Regulation of Cell Cycle Events in *Mycobacteria*: Insights From Inherently Heterogeneous Bacterial Populations. *Front Microbiol*. 2018;9. Accessed March 14, 2022. https://www.frontiersin.org/article/10.3389/fmicb.2018.00514